

Spin-orbit proximity effect in graphene on metallic substrates: decoration vs intercalation with metal adatoms

Jagoda Sławińska^{1,2,3} and Jorge I. Cerdá¹

¹*Instituto de Ciencia de Materiales de Madrid, ICMN-CSIC, Cantoblanco, 28049 Madrid, Spain*

²*Department of Solid State Physics, University of Łódź, Pomorska 149/153, 90236 Łódź, Poland*

³*Present address: Department of Physics, University of North Texas, Denton, TX 76203, USA*

(Dated: December 15, 2024)

The so-called spin-orbit proximity effect recently realized experimentally in graphene (G) on Pb/Ir(111) opens a new perspective to engineer the spin-orbit coupling (SOC) for new generation spintronics devices. Here, via large-scale density functional theory (DFT) calculations performed for two distinct graphene/metal models, G/Pt(111) and G/Au/Ni(111), we show that the spin-orbit splitting of the Dirac cones (DCs) in these structures might be enhanced by either adsorption of adatoms on top of graphene (decoration) or between the graphene and the metal (intercalation). While the decoration by inducing strong graphene-adatom interaction suppresses the linearity of the G's π bands, the intercalated structures reveal a weaker adatom-mediated graphene/substrate hybridization which preserves well-defined although broadened DCs. Remarkably, the intercalated G/Pt(111) structure exhibits a large splitting of over 100 meV, making this model a realistic candidate to confirm the previous experimental findings based on spin and angle-resolved photoemission spectroscopy.

I. INTRODUCTION

Tuning of spin-orbit coupling (SOC) in graphene¹ is one of the fundamental steps to engineer graphene-based spintronics devices. One promising route to achieve this goal is the so-called spin-orbit proximity effect, recently extensively studied from both theoretical and experimental side.²⁻⁹ This mechanism of inducing SOC extrinsically relies on the proximity between graphene (G) and a metal; the SOC of heavy atom might be *transferred* to the G when both materials are brought sufficiently close to each other. The experimental realizations of spin-orbit proximity revealed several important phenomena, such as spin Hall effect at room temperature shown by Avsar *et al*² or even more intriguing electron confinement associated to multiple topologically non-trivial gaps observed recently by Calleja *et al* in graphene on Ir intercalated by Pb nanoislands (Pb/Ir).¹⁰ While the spin-orbit proximity effect has been so far observed in rather complex structures, we believe that graphene epitaxially grown on metallic surfaces is a simple and interesting candidate material for spintronics, which not only could offer enhancing of SOC but also its tuning via the controllable adsorption or intercalation of atoms/layers of various species.

Recently, we have reported that the mechanism of inducing SOC in graphene by metallic substrates is far more complex than it had been predicted before.¹¹ Our DFT calculations of graphene on Pt(111) and on Au/Ni(111) showed that the its spin texture is a result of spin-dependent hybridization between the Dirac cones (DCs) and d bands of metal. The spin vector of graphene follows that of the substrate, thus rotates where the hybridization with spin-split metallic bands occur. The reported non-trivial spin textures, although very intriguing from the fundamental point of view, seem

difficult to control in any practical spintronics applications. Although hybridization between DCs and d states of metal may locally open mini-gaps around which the SOC-derived spin splitting reaches over 100 meV, such strong deformation of linear bands is likely to depreciate spin transport characteristics.

The main purpose of this study is to investigate several alternatives of introducing single metal adatoms with large SOC into graphene/metal interface and to explore their influence on electronic properties and spin textures of the Dirac cones. We compare two different types of adsorption which should lead to two completely different interaction models, (i) decoration defined as a simple adsorption of the adatom on top of graphene and (ii) intercalation of an adatom between the graphene and the metallic surface. Based on the spatial arrangement, the first structure should induce mainly changes in the graphene's properties, while the latter might significantly affect the graphene-substrate proximity, because graphene will interact with the metal through the intercalated adatom. We focus on two previously studied models, G/Pt(111) and G/Au/Ni(111) which, as we have shown in Ref.11, represent fundamentally different properties. In order to simplify the analysis, we consider only the adsorption of one element for each system, i.e. Pt adatom for G/Pt(111) and, analogically, Au adatom for G/Au/Ni(111). Such choice can correspond to naturally occurring defects in real samples.

The paper is organized as follows. In Sec II we provide a brief description of DFT calculations. Section III reports the electronic properties and spin textures of the G/Pt(111) calculated defect-free case and both types of adsorption. In Sec. IV we present a similar analysis for G/Au/Ni(111) structures. The conclusions are summarized in Sec. V.

II. METHODS

Our large-scale DFT calculations have been performed with the SIESTA code¹² as implemented within the GREEN package.^{13,14} The exchange-correlation (XC) potential has been treated using the generalized gradient approximation (GGA) in the Perdew, Burke, and Ernzerhof formalism.¹⁵ Spin-orbit coupling has been self-consistently taken into account as implemented in Ref. 16. Core electrons have been simulated employing norm-conserving pseudopotentials of the Troulliers-Martin type, with core corrections for the metal atoms. The atomic orbital (AO) basis set based on double-zeta polarized strictly localized numerical orbitals has been generated setting the confinement energy of 100 meV. Real space three-center integrals have been computed over 3D-grids with a resolution equivalent to 500 Rydbergs mesh cut-off, while the Brillouin zone integrations have been performed over k-supercells of around (18×18) with respect to the G- (1×1) unit cell. The temperature $K_B T$ in the Fermi-Dirac distribution has been set to 10 meV.

We have employed huge supercells to properly include moiré patterns and reconstructions (Fig.1). In case of the G/Pt(111) we considered thick slabs of Pt (6 layers) with graphene adsorbed on top and a G- (3×3) /Pt- $(\sqrt{7} \times \sqrt{7})R19.1^\circ$ moiré pattern which yields a minimal lattice mismatch.¹⁷ In order to reduce the interaction between defects in neighbouring supercells we have enlarged the (3×3) cells to a (6×6) and placed a Pt adatom either on top of the G (in an *atop* configuration) or between the G and the Pt surface (at an *fcc* site and below a C atom). Based on our previous study,¹¹ we modeled the G/Au/Ni(111) system assuming a $(9 \times 9)/(8 \times 8)/(9 \times 9)$ commensurability between the G, Au and Ni lattices, respectively, with the Au layer intercalated between the G and the four Ni layers thick slab. The Au adatoms have been incorporated either on top of the graphene (*atop*) or in between the G and the Au layer (below a C atom and above a Ni atom). The final adsorption structures have been obtained after relaxing the graphene, the adatom (when present), and the two first layers of metallic surfaces until forces were smaller than $0.04 \text{ eV}/\text{\AA}$.

Finally, the electronic structures have been evaluated in the form of projected density of states $\text{PDOS}(\vec{k}, E)$ calculated for the semi-infinite surfaces constructed after replacing the bottom layers of the slabs by a semi-infinite bulk following the Green's functions based prescription detailed in Refs. 14 and 18. Note that unfolding of the G-projected band structure into its primitive BZ is not possible in the configurations with adatoms due to the strong interaction that breaks the translation symmetry. Hence all projections are presented folded into the supercell's BZ.

III. G/PT(111): INTERCALATION VS DECORATION WITH PT ADATOMS

Figure 1 (a-c) shows the relaxed geometries of all considered G/Pt(111) structures, that is, a defect-free one in (a), the atop adsorption of single atom in (b) and the model of intercalation of the adatom between graphene and Pt(111) surface in (c). Figure 2 presents all the corresponding electronic structures and spin textures.

Let us first briefly summarize the main results obtained for the defect-free configuration. As we use a larger (6×6) supercell, the BZ shrinks and the bands backfold (DCs from K/K' are brought to Γ) which makes the analysis more difficult than in (3×3) cell corresponding to the considered moiré pattern.¹¹ However, we are still able to notice that the band structure of graphene is significantly influenced by the hybridization between DCs and Pt-*d* orbitals located close to the Fermi level despite the physisorption regime of interaction indicated by a large distance between the graphene and the metal (3.37 \AA). Indeed, in Fig. 2 (a), which presents the $\text{PDOS}(\vec{k}, E)$ of graphene (red) and Pt surface (light blue) superimposed at one map, we observe an overall blurring due to numerous anti-crossings with Pt's *d* bands; we note that their number is enhanced due to the reduced size of the BZ. Interestingly, we can still recognize the imprint of the Pt's surface state (SS) which, among other highly dispersive *sp*-like bands, crosses the upper DCs in Γ at the graphene's gap lower edge. To our surprise and despite the clear Rashba splitting (RS) of the SS, hardly any traces of DCs spin-splitting can be observed in the $\text{PDOS}(\vec{k}, E)$ map.

In Figs. 2 (b)-(c), we present spin textures projected on the G and the Pt surface, respectively. We plot simultaneously, representing by different colors, the three cartesian components of the spin polarization (s_x) green, s_y red and s_z as blue tones). Despite the complexity of the color scheme and the reduced size of the BZ, we are still able to notice that the profusion of Pt bulk bands crossing the DCs induces huge reorientations of the graphene's and substrate's spin vectors. While their origin was explained in detail in our previous work based on unfolded structures,¹¹ here we just note that the spin-splitting of the DCs is not uniform at all; we observe several mini-gaps and changes of spin direction, which suggest that such spin texture might be very difficult to control.

A. Intercalation between graphene and Pt surface

Intercalation of the Pt adatom between the graphene and the substrate induces a strong buckling of the former - the corrugation achieves a large value of 0.8 \AA with short bond lengths of 2.1 \AA between carbon and Pt_{ad} . To our surprise, the electronic structure presented in Fig. 2 (a'), consisting of superimposed bands of G (red), adatom (yellow) and Pt surface (light blue), does not reveal any

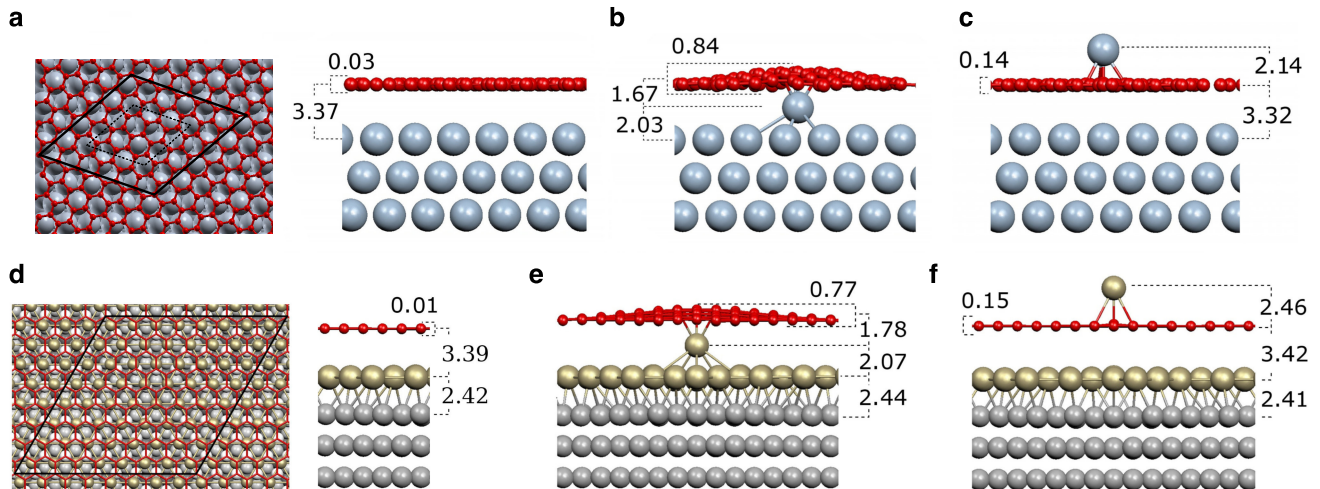


FIG. 1. (a) Top and side view of the G/Pt(111). The (3×3) supercell has been enlarged to (6×6) to avoid interactions between adatoms in configurations (b) and (c). (b) Side view of G/Pt(111) with Pt adatom intercalated between graphene and the first Pt layer. (c) Same as (b), but with Pt_{ad} placed above (on top) of a C atom in graphene. (d) Relaxed geometry of the G/Au/Ni(111) structure. (e) Same as (b) for G/Au/Ni(111). (f) Same as (c) for G/Au/Ni(111). Graphene is represented either by red balls or sticks, while Pt, Au and Ni atoms by blue, yellow and grey balls, respectively. The black parallelograms in (a) and (d) mark the $G(3 \times 3)/\text{Pt}(\sqrt{7} \times \sqrt{7})R19.1^\circ$ and $G(9 \times 9)/\text{Au}(8 \times 8)/\text{Ni}(9 \times 9)$ supercells, respectively. All distances are given in Å.

trace of localized states. Instead, the adatom contribution appears as a rather faint smudge in the PDOS (yellowish tones in the map). This can be explained by the hybridization between the intercalated atom and numerous Pt surface's and bulk's bands, which causes that the Pt_{ad} features appear more in a form of a bulklike continuum than well-defined localized states. We emphasize that without employing semi-infinite surfaces simulated via the Green's function formalism, such details would be very difficult to capture. The most important features are the changes in DCs with respect to the defect-free case. It is apparent that due to the interaction with adatom, one of the DCs vanishes while the other remain well-preserved but strongly broadened in the whole considered region. The case of the intercalation cannot be then analyzed in terms of G- Pt_{ad} and Pt_{ad} -substrate interaction separately. We would rather characterize it as a graphene-substrate interaction mediated by the adatom.

The spin structure of graphene shown in panel (b') reveals several differences with respect to the defect-free case. As can be inferred from substrate's and adatom's spin textures shown in (c') and (d'), the spin texture of G rather follows the one projected on adatom. The origin of such behavior cannot be explained in a simple way, because the PDOS of the adatom is so strongly influenced by the substrate that it is impossible to understand different fragments of the spin textures. We only observe that in the occupied part the regions of the same color lie rather horizontally along $\Gamma - K - M$ direction confirming their localized (atomic) character. In the unoccupied region, in contrast, we clearly recognize similarities with

spin texture of the substrate, including the traces of Pt's surface state.

The spin texture of G in the region where the DC is well-defined (between E_F and approximately -1.0 eV) reveals huge (over 100 meV) spin splitting of the band. Moreover, the splitting is almost constant, we do not observe any regions with abrupt anti-crossings that could cause a reorientation of the spin vector. Therefore, the splitting might be considered as more *global*, contrary to *local* splittings appearing in defect-free G/Pt(111) structure. In order to analyze it in more detail, we have plotted in Fig. 3 single spectra corresponding to spin vector vs energy ($\vec{s}(E)$) for one selected k -point. They are compared with analogical data calculated for the defect-free model and the same k -point. For occupied DC branches (left-hand panels) the spin-splitting is clearly larger in case of the intercalated model, although the interaction with the adatom significantly broadens the PDOS. We note that even at the unoccupied energies, despite the Pt_{ad} are apparently absent, the intercalation induces much larger values of spin-splitting (e.g. for the first DC branch the splitting increases from around 10 meV to over 50 meV). Thus, in our opinion, intercalation might be quite efficient way to enhance spin-orbit proximity effect.

Finally, we would like to remark, that our results for intercalated model agree quite well with experimental findings revealed by spin- and angle-resolved photoemission spectroscopy (SP-ARPES) for G/Pt(111).^{19,20} Although it was suggested that the measured giant splitting (~ 100 meV) was induced by the Pt(111) surface, it was

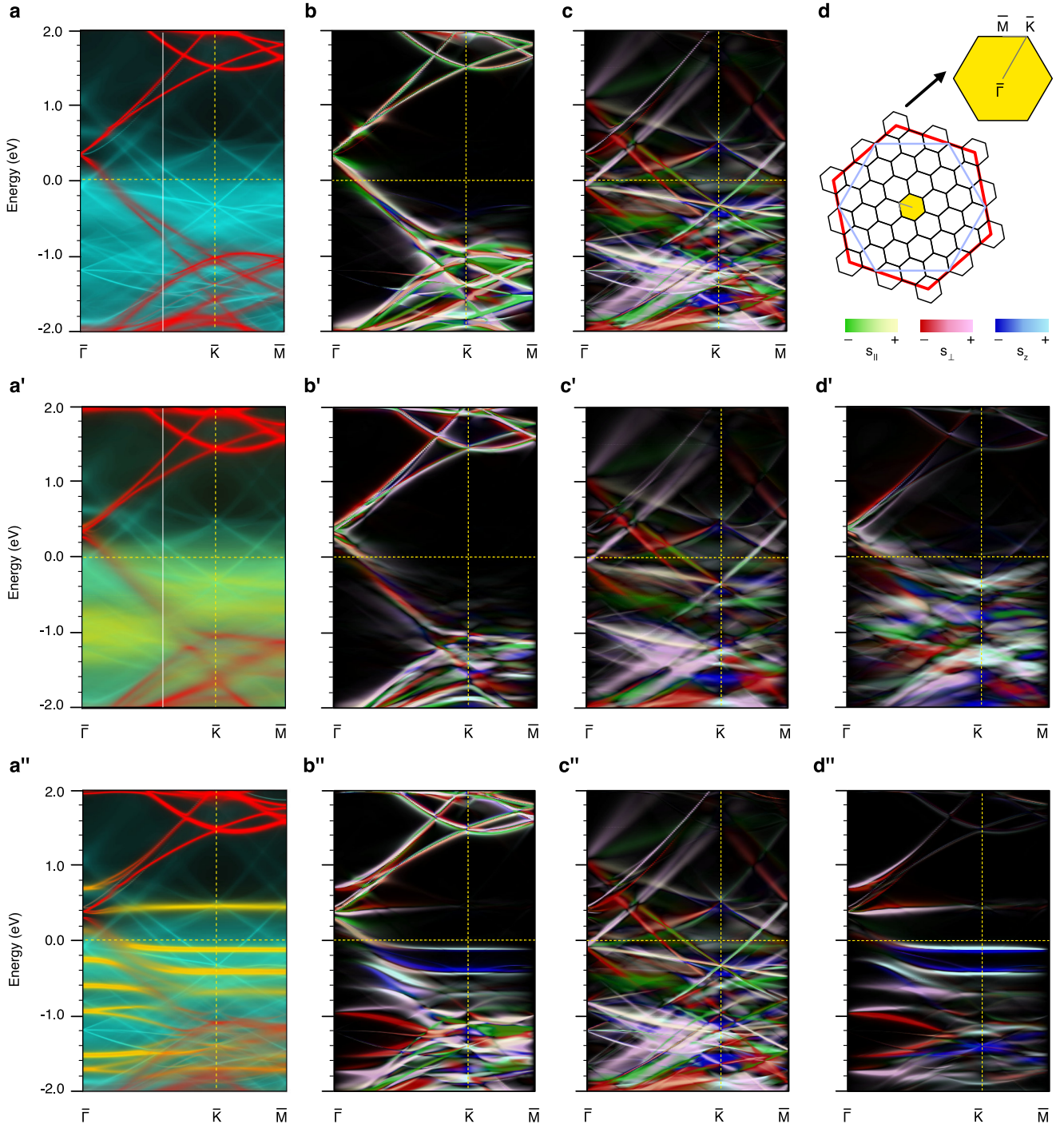


FIG. 2. Electronic and spin structure of G/Pt(111) intercalated/decorated with single Pt atoms. (a) Density of states of G/Pt(111) calculated in (6×6) supercell and projected on graphene (red) and Pt (light-blue). (b) Corresponding spin texture projected on graphene. The color scheme is defined as follows: green/red shades refer to the direction of spin parallel/perpendicular to the momentum, while blue corresponds to the out-of-plane component; light/dark tones denotes positive/negative values of each component, see also the inset summarizing the legends in the bottom of panel (d). (c) Same as (b) projected on Pt substrate. (d) Brillouin zones of the (6×6) supercell (small black hexagons), G- (1×1) primitive cell (red hexagon), and Pt- (1×1) primitive cell (blue hexagon). The selected k -lines are marked within the yellow hexagon in the center. (a'-c') Same as (a-c) for the configuration with intercalated Pt atom; its PDOS in (a') is colored in yellow, and its spin texture is displayed in (d'). (a''-d'') Same as (a'-d') for configuration with single Pt atoms adsorbed on top of G.

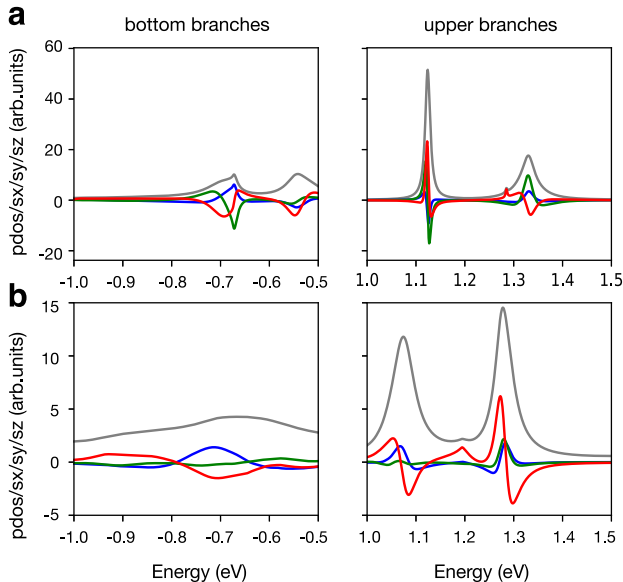


FIG. 3. PDOS(E) and $\vec{s}(E)$ single spectra extracted from the maps in Fig.2 (a)-(a') at specific k-point marked with white dashed line. Panel (a) corresponds to the defect free case and (b) to the intercalated model. Left-hand (right-hand) panel shows occupied (unoccupied) DC branches. Grey, red, green and blue lines represent the PDOS, and s_{\perp} , s_{\parallel} and s_z components of \vec{s} , respectively.

not confirmed by theoretical calculations. The intercalated model seems to capture the experimental results (broadening and huge spin-splitting) much better than just the G/Pt(111) interface. As such intercalations are likely to occur in real samples, we are convinced that it might be a possible explanation of the unusual enhancing of SOC.

B. Pt adsorption on top of G/Pt(111)

Contrary to the intercalation case, the adsorption of Pt adatom on top of G/Pt(111) leads to hardly any buckling of the G - the corrugation does not exceed 0.1 Å (see Fig. 1). However, a very short distance between the adatom and the G (2.14 Å) induces a strong interaction and several changes in the electronic structure of graphene, as can be easily noticed in Fig. 2 (a'') where the PDOS(\vec{k}, E) of G, Pt_{ad} and Pt(111) are superimposed. The most striking feature is a bunch of intense localized bands of the adatom (yellow) which completely tear the lower DCs and notably alter the upper ones. Such picture can be easily explained with the help of simpler model consisting of just graphene and adatom (G+Pt_{ad}). The PDOS of such configuration (see Fig.S1(a) in the Supplementary Material) strongly resembles the one presented here in panel (a''), and suggests that the only effect of G/substrate interaction would be the p -type doping of

over 300 meV. The adatom's states in the occupied region reveal mainly $5d$ character. Only one band at approximately +400 meV which directly crosses the Dirac point (DP) has an sp origin.

The spin textures of G, Pt(111), and Pt_{ad} are shown in panels (b''-d''). As expected on the base of the previous works which dealt with simple models of adsorption on top of freestanding graphene,^{9,10,21,22} indeed the adatom induces large splitting in the graphene's π bands. It can be explained comparing the spin texture of graphene with that of the adatom. The hardly dispersive quasi-atomic states at around -100, -400 and -600 meV are significantly splitted and, due to the extended regions of hybridization, their spin texture is directly reflected in the graphene's π bands which are endowed with the splittings of up to 200 meV. Interestingly, the spin textures of graphene and the adatom in the simpler G+Pt_{ad} model (Fig.S1b-c) do not explain the complicated spin dependent interaction image of Fig. 2 (b''), clearly indicating that a weakly interacting substrate largely impacts the final spin polarization of the graphene's bands. Also in the regions where the localized Pt_{ad} states are not present, the spin structure of the substrate is a dominant factor in formation of graphene's DCs spin texture. It occurs e.g. above +1.5 eV where G's spin structure resembles the complicated image of defect-free G/Pt(111).

IV. ADSORPTION OF SINGLE AU ADATOMS IN G/AU/NI(111)

Figure 4 summarizes the electronic and spin structures of all considered G/Au/Ni(111) models. Let us first address the defect-free case whose properties are displayed in panels (a)-(c). Weak graphene-Au interaction,²³⁻²⁷ which leaves an uncorrugated graphene layer at 3.4 Å above the substrate, manifests in almost undoped and well-preserved DCs up to the binding energies of around -1 eV, fully confirming its quasi-freestanding character reported in numerous previous works.^{21,28,29} In the combined PDOS(\vec{k}, E) map (a) consisting of projected G (red), Au (light blue) and Ni surface (dark blue), the features corresponding to the latter are located at approximately -0.7 (+0.2) eV, and represent the upper part of the majority (minority) d -bands. The sp bands of Au (the most prominent of them a Shockley-type surface state^{16,30} emerging from Γ at -0.33 eV) cross the BZ at several energies whereas weak fingerprints of the Au $5d$ -bands (light blue) appear below -1 eV largely distorting the graphene's DCs. Overall, the hybridization between graphene and the underlying Au/Ni(111) is much weaker than in G/Pt(111) structure, suggesting that this system might be easier to control in practice.

In spite of the fact that the properties of the system are fundamentally different from G/Pt models (now we deal with an interplay of SOC and exchange interaction), the spin texture of graphene shown in Fig. 4 (b) appears less complex than in the G/Pt(111). First of all, we notice

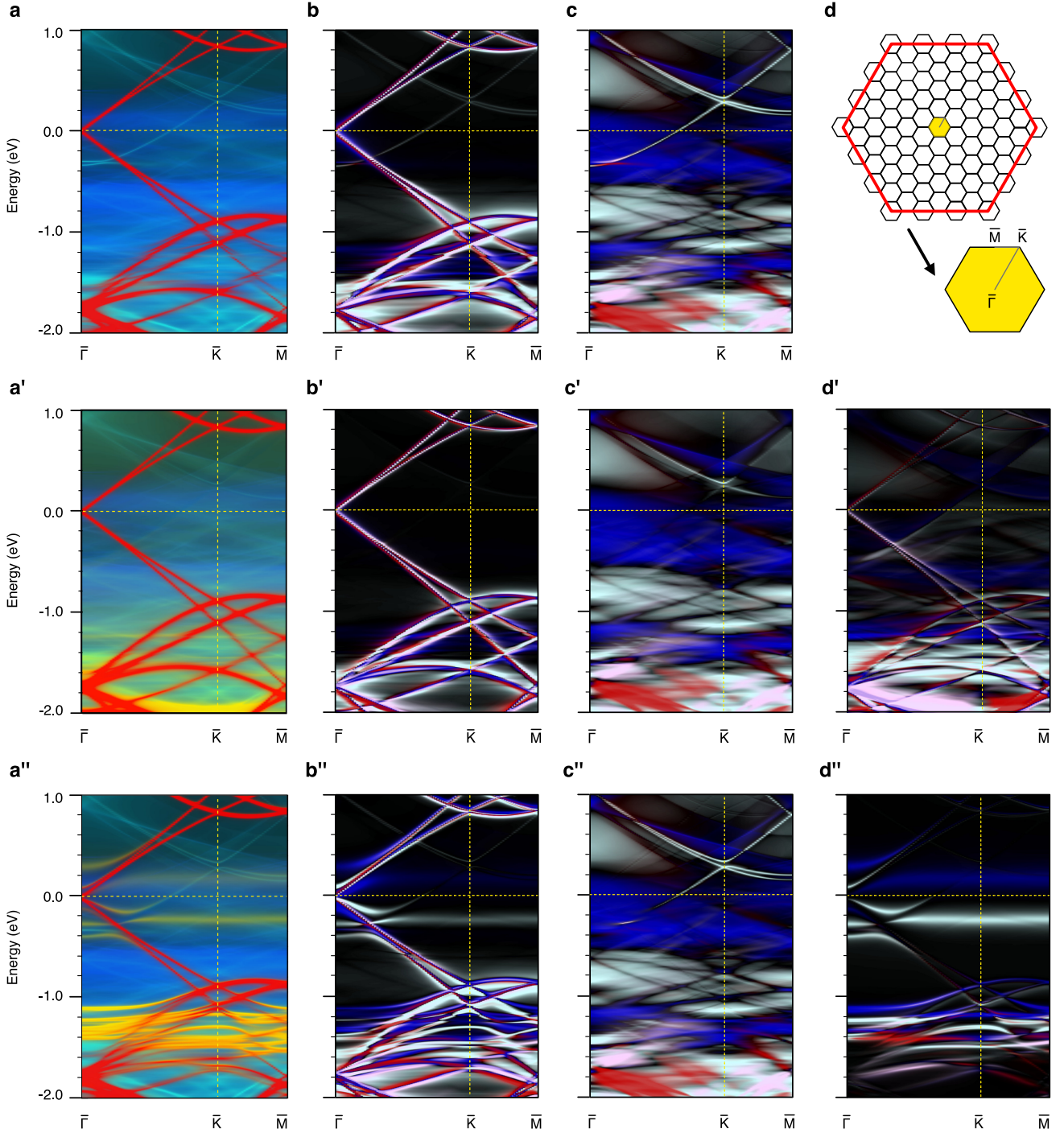


FIG. 4. Electronic and spin structure of G/Au/Ni(111) intercalated/decorated with single Au atoms. (a) Band structure of G/Au/Ni(111) along $\Gamma - K - M$ in folded (9×9) BZ represented as $\text{PDOS}(\vec{k}, E)$ projected on graphene (red), gold (light blue) and Ni surface (dark blue) superimposed at one map. (b) Corresponding graphene's spin texture after superimposing the $x/y/z$ components, each color coded as explained in Fig.2. (c) Same as (b), but projected on intercalated Au layer. (d) Brillouin zones of the (9×9) supercell (small black hexagons), and G- (1×1) primitive cell (red hexagon); the considered k -lines are labeled within the yellow hexagon. (a'-c') Same as (a-c) for the configuration with additional Au atom intercalated below the G; yellow shades in (a') denote its PDOS, while panel (d') shows its spin texture. (a''-d'') Same as (a'-d') for the configuration of G/Au/Ni(111) with Au atoms adsorbed on top of the G. The spin textures projected on Ni(111) are neglected in all cases.

that the spin vector has only components perpendicular to the momentum (in-plane and out-of-plane). As it has been explained in Ref. 11 with the help of unfolded projection onto G-(1×1) primitive cell, the spin texture originates mainly from exchange-split bands of Ni hybridized with Au $5d$ states. Although the spin texture of Ni has been omitted in Fig. 4, the spin polarized Ni(111) bands, due to a strong hybridization with Au interlayer, are clearly visible in the spin texture of the latter (c) in the form of light and dark blue regions representing spin majority and minority, respectively. SOC manifests most notably in the lower energy region (below -1.0 eV), where in-plane components can be clearly seen at several energies; here the interaction with Au involves, apart from the G's linear branches, also nonlinear parts of π bands backfolded and crossing the DCs at K .

We again explored the role of adatoms either adsorbed above the graphene or intercalated between the graphene and the Au monolayer. The relaxed structures, shown in Figs. 1 (e)-(f), essentially follow the same geometrical trends as in the G/Pt system. The intercalated adatom induces a significant buckling in the G (0.77 Å); moreover, it increases a distance between the G and the Au monolayer. In contrast to intercalated G/Pt(111) structure, an additional Au atom incorporated below graphene in G/Au/Ni(111) (a') introduces only some subtle changes in the band structure (e.g. removal of the SS of Au) leaving the graphene's DCs hardly affected. The spin texture (b') is very similar to the one in defect-free model (b), the only difference are vanishing exchange-split Ni bands, which can be attributed to the larger distance between G and the Ni(111). The lack of additional features due to the adatom, despite it exhibits a non-trivial spin texture (d'), can be assigned to a weak hybridization between the DCs and adatom's bands, easily seen even in the PDOS map. The adatom's states, in contrast to G/Pt case, are not very intense and cross the DCs at lower energies (below -1.0 eV). Moreover, due to a larger distance between G and Ni(111) they mix less with the bulk bands and resemble localized states similar to those induced by just an adatom (see Fig.S2 in SM). As a result, in case of the G/Au/Ni(111) intercalation of an Au adatom does not enhance the SOC derived spin splitting, suggesting that the mechanism described in the previous section strongly depends on the metal (the position of d bands, hybridization between intercalated atom and the surface, etc.)

Similarly to G/Pt(111), when Au_{ad} is introduced on top of the G, the graphene remains hardly corrugated (0.15 Å), although the $C-Au_{ad}$ bond becomes very short (2.46 Å). The atomic metal d states (intense yellow) strongly hybridize with DCs opening multiple gaps which completely destroy its linearity below -1 eV and perturb it in the regions close to E_F . Following the strategy employed in case of G/Pt we have additionally considered a simpler G+ Au_{ad} model. Again, the PDOS presented in Fig.S2a reveals a negligible role of the substrate in the graphene's electronic properties - it does not even induce

any doping as the G is quasi-freestanding at Au/Ni(111). The only difference is the position of one of Au_{ad} localized states which has been splitted due to the exchange interaction. Its lower part shifted from the Fermi level to around -300 meV slightly tears the graphene's DCs. The adatom's spin texture (d'') further confirms the exchange splitting of this state absent in the model neglecting the substrate (Fig.S2c). The induced splitting of the DC is, however, very local and, obviously, of purely out-of-plane character confirming its exchange, instead of SOC origin which could be deduced from just G+ Au_{ad} model. Although other features of the adatom's spin texture, mainly below -1.0 eV, reveal a weak SOC character, it is quite difficult to estimate the SOC of graphene induced by those particular Au_{ad} bands, similarly as in the defect-free G/Au/Ni(111). Overall, only the exchange splitting is larger here than in the configuration without adatoms; DCs are perturbed only very close to the Fermi level and significantly less than in the G/Pt(111) decorated by Pt adatom. Finally, we remark that none of the presented G/Au/Ni(111) models can explain a giant phase spin-splitting reported in Ref.21. We believe that a further study, employing a model based on the formation of Ni/Au alloy at the surface region (similar to one reported for the G/Fe/Ir(111) system³¹) might provide a more suitable description of these experiments.

V. SUMMARY AND CONCLUSIONS

We have investigated the spin-orbit proximity effect in graphene on metallic substrates decorated or intercalated by metallic adatoms. We have focused on two specific graphene/metal models, non-magnetic G/Pt(111) and magnetic G/Au/Ni(111), both previously studied experimentally.^{19,21} We have focused on the influence of metal adatoms in these systems (Pt and Au, respectively) showing two very different scenarios depending on the location of the defect; we have found that adsorption on top of graphene leads to a densely teared Dirac cones due to hybridizations with the atomic-like states, resembling freestanding graphene decorated by adatoms. On the other hand, when intercalated between the graphene and the metal surface the adatom's states strongly hybridize with the substrate's continuum of bands and the graphene's π bands are not visibly affected.

The major findings are the spin textures of all considered structures relevant for understanding of SOC proximity effect in graphene. The most intriguing system is the Pt-intercalated G/Pt(111) which reveals a large spin-orbit derived spin-splitting of around 100 meV present within a wide energy range between E_F and approximately -1 eV. We believe that such an intercalation could be an origin of observed giant spin-orbit splitting in graphene epitaxially grown on Pt studied via SP-ARPES in Ref. 19. We emphasize, however, that the resulting DC is broadened due to the hybridization with Pt_{ad} -Pt(111) bands. In case of G/Au/Ni(111), in contrast,

we have found that the SOC-derived splitting of the DCs can be enhanced only by decoration with adatoms on top of graphene which is, however, accompanied by the loss of linearity of the π bands.

In conclusion, we have found that the intercalation of graphene-based structures is a more promising route of enhancing SOC than the adsorption of adatoms on top of graphene. We are convinced that our results will stimulate further experimental studies of SOC in epitaxial graphene, which could be tuned via low-coverage intercalation of various species between the graphene and a

metallic substrate.

ACKNOWLEDGMENTS

J.S. acknowledges Polish Ministry of Science and Higher Education for the Mobility Plus Fellowship (Grant No. 910/MOB/2012/0). J.I.C acknowledges support from the Spanish Ministry of Economy and Competitiveness under contract No. MAT2015-66888-C3-1R. Part of the calculations have been done in the supercomputer MareNostrum at Barcelona Supercomputing Center.

-
- ¹ W. Han, R. K. Kawakami, M. Gmitra, and J. Fabian, *Nature Nanotech.* **9**, 794 (2014).
- ² A. Avsar, J. Y. Tan, T. Taychatanapat, J. Balakrishnan, G. Koon, Y. Yeo, J. Lahiri, A. Carvalho, A. S. Rodin, E. O-Farrell, G. Eda, A. H. C. Neto, and B. Ozyilmaz, *Nat. Commun.* **5**, 4875 (2014).
- ³ S. Irmer, T. Frank, S. Putz, M. Gmitra, D. Kochan, and J. Fabian, *Phys. Rev. B* **91**, 115141 (2015).
- ⁴ C. Weeks, J. Hu, J. Alicea, M. Franz, and R. Wu, *Phys. Rev. X* **1**, 021001 (2011).
- ⁵ M. Gmitra and J. Fabian, *Phys. Rev. B* **92**, 155403 (2015).
- ⁶ A. M. Shikin, A. G. Rybkin, D. Marchenko, A. A. Rybkina, M. R. Scholz, O. Rader, and A. Varykhalov, *New Journal of Physics* **15**, 013016 (2013).
- ⁷ Z. Y. Li, Z. Q. Yang, S. Qiao, J. Hu, and R. Q. Wu, *Journal of Physics: Condensed Matter* **23**, 225502 (2011).
- ⁸ J. Balakrishnan, G. K. W. Koon, A. Avsar, Y. Ho, J. H. Lee, M. Jaiswal, S.-J. Baeck, J.-H. Ahn, A. Ferreira, M. A. Cazalilla, A. H. C. Neto, and B. Ozyilmaz, *Nat. Commun.* **5**, 4748 (2014).
- ⁹ D. Ma, Z. Li, and Z. Yang, *Carbon* **50**, 297 (2012).
- ¹⁰ F. Calleja, H. Ochoa, M. Garnica, S. Barja, J. J. Navarro, A. Black, M. M. Otrokov, E. V. Chulkov, A. Arnau, A. L. Vazquez de Parga, F. Guinea, and R. Miranda, *Nature Phys.* **11**, 43 (2015).
- ¹¹ J. Sławińska and J. I. Cerdá, *Phys. Rev. B* **98**, 075436 (2018).
- ¹² J. M. Soler, E. Artacho, J. D. Gale, A. Garcia, J. Junquera, P. Ordejon, and D. Sanchez-Portal, *Journal of Physics: Condensed Matter* **14**, 2745 (2002).
- ¹³ J. Cerdá, M. A. Van Hove, P. Sautet, and M. Salmeron, *Phys. Rev. B* **56**, 15885 (1997).
- ¹⁴ E. T. R. Rossen, C. F. J. Flipse, and J. I. Cerdá, *Phys. Rev. B* **87**, 235412 (2013).
- ¹⁵ J. P. Perdew, K. Burke, and M. Ernzerhof, *Phys. Rev. Lett.* **77**, 3865 (1996).
- ¹⁶ R. Cuadrado and J. I. Cerdá, *Journal of Physics: Condensed Matter* **24**, 086005 (2012).
- ¹⁷ P. Merino, M. Svec, A. L. Pinardi, G. Otero, and J. A. Martin-Gago, *ACS Nano* **5**, 5627 (2011).
- ¹⁸ C. Rogero, J. A. Martin-Gago, and J. I. Cerdá, *Phys. Rev. B* **74**, 121404 (2006).
- ¹⁹ A. M. Shikin, A. A. Rybkina, A. G. Rybkin, I. I. Klimovskikh, P. N. Skirdkov, K. A. Zvezdin, and A. K. Zvezdin, *Applied Physics Letters* **105**, 042407 (2014).
- ²⁰ I. I. Klimovskikh, S. S. Tsirkin, A. G. Rybkin, A. A. Rybkina, M. V. Filianina, E. V. Zhizhin, E. V. Chulkov, and A. M. Shikin, *Phys. Rev. B* **90**, 235431 (2014).
- ²¹ D. Marchenko, A. Varykhalov, M. Scholz, G. Bihlmayer, E. Rashba, A. Rybkin, A. Shikin, and O. Rader, *Nat Commun* **3**, 0 (2013).
- ²² S. Abdelouahed, A. Ernst, J. Henk, I. Maznichenko, and I. Mertig, *Phys. Rev. B* **82**, 125424 (2010).
- ²³ G. Giovannetti, P. A. Khomyakov, G. Brocks, V. M. Karpan, J. van den Brink, and P. J. Kelly, *Phys. Rev. Lett.* **101**, 026803 (2008).
- ²⁴ Z. Klusek, P. Dabrowski, P. Kowalczyk, W. Kozłowski, W. Olejniczak, P. Blake, M. Szybowicz, and T. Runka, *Applied Physics Letters* **95**, 113114 (2009).
- ²⁵ J. Sławińska, P. Dabrowski, and I. Zasada, *Phys. Rev. B* **83**, 245429 (2011).
- ²⁶ J. Sławińska, I. Wlasny, P. Dabrowski, Z. Klusek, and I. Zasada, *Phys. Rev. B* **85**, 235430 (2012).
- ²⁷ T. Olsen and K. S. Thygesen, *Phys. Rev. B* **87**, 075111 (2013).
- ²⁸ A. Varykhalov, J. Sánchez-Barriga, A. M. Shikin, C. Biswas, E. Vescovo, A. Rybkin, D. Marchenko, and O. Rader, *Phys. Rev. Lett.* **101**, 157601 (2008).
- ²⁹ A. Varykhalov, J. Sanchez-Barriga, A. M. Shikin, C. Biswas, E. Vescovo, A. Rybkin, D. Marchenko, and O. Rader, *Phys. Rev. Lett.* **101**, 157601 (2008).
- ³⁰ S. LaShell, B. A. McDougall, and E. Jensen, *Phys. Rev. Lett.* **77**, 3419 (1996).
- ³¹ J. Brede, J. Sławińska, M. Abadia, C. Rogero, J. E. Ortega, I. Piquero-Zulaica, J. Lobo-Checa, A. Arnau, and J. I. Cerdá, *2D Materials* **4**, 015016 (2017).